

February 4, 2002

Search

## Centimeter-Accuracy Indoor Navigation Using GPS-Like Pseudolites

November 1, 2001

By: [Changdon Kee](#), [Doohee Yun](#), [Haeyoung Jun](#), [Bradford Parkinson](#), [Sam Pullen](#), [Tom Lagenstein](#)  
GPS World

 [E-mail This Article](#)

### Advanced Search

[About the Magazine](#)

[GPS World](#)

[Media Kit](#)

[Subscribe](#)

[Contact](#)

[Meet the Staff](#)

[Editorial Board](#)

[Services](#)

[From The Editor](#)

[GPS News](#)

[Global View](#)

[GPS Inside](#)

[Leading Edge](#)

[GPS Products](#)

[New Products](#)

[Buyers Guide](#)

[LeadNet](#)

[Calendar](#)

[GPS Jobs](#)

[GPS Reference](#)

[Galileo's World](#)



Figure 1 Schematic overview of indoor navigation system using pseudolites

Use of GPS pseudolites now makes it possible to apply GPS navigation in an indoor environment. A pseudolite is a signal generator that transmits GPS-like signals to nearby users. In the United States, interest in pseudolite-based indoor navigation stems in part from imminent implementation of new automatic location capability in mobile cellular phones - so-called Enhanced 911 or E911 - required by a new Federal Communications Commission (FCC) rule.

With this motivation, in 1999 the Seoul National University GPS Lab (SNUGL) developed a centimeter-accuracy indoor navigation system using asynchronous pseudolites. The system has been upgraded in the last year to include carrier phase cycle-slip recovery and automatic cycle ambiguity-resolution functions. Using this system as a position and attitude sensor, SNUGL implemented a vehicle control system and obtained 1-2 centimeter control errors. These results demonstrated that, if pseudolites are used, GPS navigation is possible in indoor environments, such as a large factory, indoor amusement park, or anywhere GPS signals are blocked.



Figure 2 The indoor testbed

We are convinced that our research results and use of this approach will help pioneer the extension of GPS navigation into the indoor world. This article describes the pseudolite-based positioning techniques and their application to track and control a miniature vehicle operating on an indoor track.



Table 1

**Indoor Navigation** The SNU indoor navigation system incorporates pseudolites, a reference station, and a user vehicle. Figure 1 shows an overview of the system. As shown in the figure, the pseudolites are fixed; so, their positions can be calibrated off-line. To calculate pseudolite positions, we used carrier-phase measurements and applied inverse carrier phase differential GPS (ICDGPS).

We use an algorithmic methodology developed at SNUGL and discussed in a paper presented at the U.S. Institute of Navigation (ION) GPS-1999 conference ("Precise Calibration of Pseudolite Positions In Indoor Navigation System") to accurately determine the positions of the fixed pseudolites. We have verified by simulation that this algorithm can calculate the phase center of each pseudolite antenna with millimeter-level accuracy. The reference station is also fixed at the floor and transmits carrier phase corrections to the user by means of a wireless datalink. Applying these corrections, the user calculates its position using carrier phase differential GPS (CDGPS). This approach is fundamentally similar to outdoor CDGPS. However, an indoor navigation system is more difficult to implement due to a near/far problem in which the received power from nearby transmitters is stronger than those from more distant ones and acts as an interfering source. We also needed to operate under serious multipath (reflected signals) conditions and had to devise a method for synchronizing the pseudolites' timing, which is based on temperature-compensated crystal oscillators (TXCOs).

Stanford University developed an indoor navigation experiment using pseudolites about five years ago and suggested some solutions that are discussed in papers included in the "Further Readings" section at the end of this article. Stanford also

applied pseudolites to open-pit mining about three years ago.

With some insights from these results, SNUGL was the first in Asia to successfully develop a more robust and practical indoor navigation system (first demonstrated in October 1999) and has continued to upgrade the system. We have implemented the indoor navigation system in the space of about 53533 meters, as shown in Figure 2. We installed a "master" pseudolite in the center of the ceiling and used its navigation message to synchronize the receiver's sampling time. We analyzed the positioning performance of our indoor navigation system by use of a mobile miniature train and summarized the results in Table 1.



Table 2

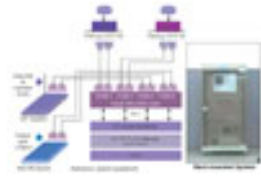


Figure 3 Schematic view and photo of the pseudolite reference station setup

**Pseudolite and Antenna Calibration** We used commercial pseudolites and configured the navigation message to eliminate information content and produce a 50-bps data stream that is used only for bit and frame lock. To solve the near/far problem, we tuned the pseudolite signal power and also adopted a pulsing scheme, which was discussed in an ION GPS-2000 paper ("Development of Indoor Navigation System using Asynchronous Pseudolites"). To mitigate the multipath conditions inside our laboratory, we controlled the gain patterns of the pseudolite antennas. We used hand-made helical antennas as shown in Figure 1 and set the transmission patterns as wide HPBW (Half Power Beam Width) for the master antenna and narrow for the other antennas.

Under outdoor conditions, a GPS receiver obtains almanac and ephemeris data with which to compute the position of the GPS satellites. For an indoor navigation system, we must accurately measure the positions of the transmission antennas and provide this information to users. A small error in transmitter position creates a relatively large line-of-sight vector error because of the very short distances between users and pseudolites. So, we must accurately measure the position of the phase center of the pseudolite antennas; however the shape and size of the helical antennas make it almost impossible to determine where the phase center is using only our eyes and a tape measure.



Figure 4 Operational overview of indoor navigation system

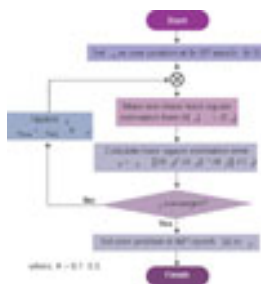


Figure 5 Nonlinear least-squares estimation of user position

To solve for the phase-center locations, we applied the ICDGPS method discussed earlier. We marked more than eight points of known positions on the lab floor and collected carrier-phase measurements at all of these points. Using the algorithm described in our ION GPS-2000 paper, we calibrated the positions of the phase center of the transmission antennas. Table 2 summarizes the results of this calibration.

**Receiver Sampling Synchronization** Our pseudolites use TCXO frequency standards, which are not very stable compared to the atomic clocks on board GPS satellites. Thus, indoor receivers cannot synchronize their sampling times to the degree possible when tracking GPS satellites outdoors. The different sampling times also introduce range errors because pseudolite clock biases, which are induced from TCXOs, drift continuously.

In order to synchronize the sampling times of reference and user receivers, we modified the receivers to adjust their sampling times to the data-message frame of the master pseudolite. Using this method, we can synchronize the sampling times to within one microsecond (1 ms), and the time-tag range error is reduced to below 0.3 millimeters, which is negligible. We used two identical 12-channel single-frequency GPS receivers, which are modified to track pseudolite signals and to synchronize their sampling times using the navigation message frame from the master pseudolite. We used only carrier-phase measurements. Thus, our indoor navigation positions are CDGPS solutions.

$$\text{Equation 1}$$

Equation 1

**Reference Station** Figure 3 shows the reference station and its equipment. The reference station has two GPS receivers, a computer, a wireless data modem, an uninterruptible power supply, and other devices. The computer operates the monitoring program, which is a key component of the indoor navigation system. The monitoring program calculates the user's position at 10 Hz and generates control commands for the miniature vehicle. SNUGL developed

this program using Microsoft Visual C++. Figure 4 shows its structure and a sample screen capture.

$$\begin{bmatrix} \Delta \phi_{12} \\ \Delta \phi_{13} \\ \Delta \phi_{14} \\ \Delta \phi_{23} \\ \Delta \phi_{24} \\ \Delta \phi_{34} \end{bmatrix} = \begin{bmatrix} \lambda \Delta \theta_{12} \\ \lambda \Delta \theta_{13} \\ \lambda \Delta \theta_{14} \\ \lambda \Delta \theta_{23} \\ \lambda \Delta \theta_{24} \\ \lambda \Delta \theta_{34} \end{bmatrix} + \begin{bmatrix} \lambda N_{12} \\ \lambda N_{13} \\ \lambda N_{14} \\ \lambda N_{23} \\ \lambda N_{24} \\ \lambda N_{34} \end{bmatrix} + \begin{bmatrix} \lambda \Delta \theta_{12} \\ \lambda \Delta \theta_{13} \\ \lambda \Delta \theta_{14} \\ \lambda \Delta \theta_{23} \\ \lambda \Delta \theta_{24} \\ \lambda \Delta \theta_{34} \end{bmatrix} + \begin{bmatrix} \lambda N_{12} \\ \lambda N_{13} \\ \lambda N_{14} \\ \lambda N_{23} \\ \lambda N_{24} \\ \lambda N_{34} \end{bmatrix}$$

Equation 2

**Ambiguity Resolution, Point Positions** As with carrier phase tracking that uses GPS satellites, the receivers used in indoor positioning are subject to ambiguities in the number of cycles in the transmissions from the pseudolites.

"Slips" in the signal tracking and data processing also can cause the receiver to lose its count of the number of elapsed cycles. Consequently, we have implemented carrier-phase cycle-slip recovery and automatic cycle ambiguity-resolution functions in the monitoring program to make our indoor navigation system more robust and practical. To accomplish this, we have developed an algorithm that resolves cycle ambiguities automatically to produce point positions.

At a given k-th epoch, the double-differenced carrier-phase measurements can be expressed as shown in Equation 1.

To resolve carrier phase integer cycle ambiguities, we make use of Equation 2, a multi-epoch version of Equation 1.

The indoor monitoring program collects 20 epochs of data and then applies non-linear least-squares estimation to resolve the cycle ambiguities. Estimated cycle ambiguities are rounded off to the nearest integers to conserve the integer characteristics. Once cycle ambiguities are determined, they remain constant until cycle slips occur. We can thus calculate the user's position on the next epoch by applying non-linear least-squares estimation to Equation 3 as shown in Figure 5.

$$\begin{bmatrix} \Delta \phi_{12} \\ \Delta \phi_{13} \\ \Delta \phi_{14} \\ \Delta \phi_{23} \\ \Delta \phi_{24} \\ \Delta \phi_{34} \end{bmatrix} = \begin{bmatrix} \lambda \Delta \theta_{12} \\ \lambda \Delta \theta_{13} \\ \lambda \Delta \theta_{14} \\ \lambda \Delta \theta_{23} \\ \lambda \Delta \theta_{24} \\ \lambda \Delta \theta_{34} \end{bmatrix} + \begin{bmatrix} \lambda N_{12} \\ \lambda N_{13} \\ \lambda N_{14} \\ \lambda N_{23} \\ \lambda N_{24} \\ \lambda N_{34} \end{bmatrix} + \begin{bmatrix} \lambda \Delta \theta_{12} \\ \lambda \Delta \theta_{13} \\ \lambda \Delta \theta_{14} \\ \lambda \Delta \theta_{23} \\ \lambda \Delta \theta_{24} \\ \lambda \Delta \theta_{34} \end{bmatrix} + \begin{bmatrix} \lambda N_{12} \\ \lambda N_{13} \\ \lambda N_{14} \\ \lambda N_{23} \\ \lambda N_{24} \\ \lambda N_{34} \end{bmatrix}$$

$\Rightarrow H(x) = z - Z(x)$   
 where  $z_k = \begin{bmatrix} \Delta \phi_{12} \\ \Delta \phi_{13} \\ \Delta \phi_{14} \\ \Delta \phi_{23} \\ \Delta \phi_{24} \\ \Delta \phi_{34} \end{bmatrix}$   
 $Z = \begin{bmatrix} \lambda \Delta \theta_{12} \\ \lambda \Delta \theta_{13} \\ \lambda \Delta \theta_{14} \\ \lambda \Delta \theta_{23} \\ \lambda \Delta \theta_{24} \\ \lambda \Delta \theta_{34} \end{bmatrix}$

Equation 3

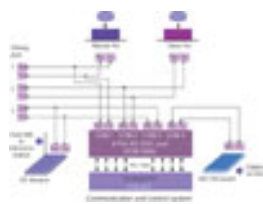


Figure 6 Miniature vehicle and communication/control system

If a cycle slip occurs after cycle-ambiguity resolution, we have to recalculate the cycle ambiguities. However, if the cycle slip occurs while signals are still being received from more than three pseudolites, the current position can be obtained; we can recalculate the "slipped" cycle ambiguities directly from the current position information and thus remove the effect of the cycle slip. This is known as "cycle-slip recovery." We implemented this function in the monitoring program, and it has added integrity to our indoor navigation system and has made it more robust in practice.

**Indoor Vehicle Operations** SNUGL constructed an autonomous indoor navigation "user" based on a miniature vehicle. Figure 6 shows the miniature vehicle and its communication/control system. To calculate two-dimensional attitude angles, we installed two GPS antennas on the vehicle's roof separating them by 36 centimeters. For autonomous operation, we equipped this vehicle with an industrial PC, a wireless data modem, and a microcontroller. The microcontroller generates pulse width modulation (PWM) servo control signals according to control commands, which are transmitted from the reference station and updated at 10 Hz.

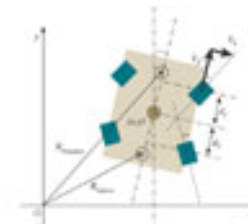


Figure 7 Modeling of the miniature vehicle

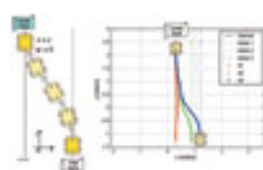


Figure 8 Line transfer control of the vehicle

Miniature Vehicle Navigation and Attitude Determination. If we used the known baseline length to calculate the user vehicle's position and attitude, the indoor navigation algorithm became too highly non-linear to solve easily. So, we decided to use a simpler method that calculates the vehicle's position by averaging point positions of the master and slave antennas. We used the point-positioning algorithm shown in Figure 5.

The vehicle's two-dimensional attitude angle is easily determined by calculating the horizontal direction of the baseline vector. To resolve cycle ambiguities, the monitoring program accumulates carrier-phase measurements until an observability condition is satisfied and then calculates cycle ambiguities using least-squares estimation. The static test results are summarized in Table 3.



Table 3

Modeling the Miniature Vehicle. Figure 7 shows all the notations used in the modeling of the miniature vehicle. The exact model of this vehicle is non-linear. As it is not easy to design non-linear controllers, we linearized the model and obtained Equation 4. If the non-linear model is linearized, modeling errors are unavoidable. However, this was not a problem because we designed the controller as a closed-loop system. In other words, we fed back the vehicle's

$$\begin{aligned} \dot{x} &= V_f \psi + V_f \delta \\ \dot{y} &= V_f - V_f \delta \psi \\ \dot{\psi} &= \frac{V_f}{d_t} \delta \end{aligned}$$

Equation 4

Controlling the Vehicle. Simple line transfer control is designed to make vehicle track a straight line defined by  $x = c$  with a 0-deg attitude angle, as shown in Figure 8. To design this controller, we defined a new variable ( $x_{new}$ ) as  $x - c$  and discretized Equation 4 into Equation 5. The sampling time ( $Dt$ ) is 0.1 sec because position and attitude are updated at 10 Hz. We used a discrete linear quadratic regulator (DLQR) method to design the controller, and the control input was calculated as Equation 6.

$$\begin{bmatrix} x_{new}(k+1) \\ \psi(k+1) \end{bmatrix} = \begin{bmatrix} 1 & V_f \Delta t \\ 0 & 1 \end{bmatrix} \begin{bmatrix} x_{new}(k) \\ \psi(k) \end{bmatrix} + \begin{bmatrix} V_f \\ V_f / d_t \end{bmatrix} \Delta t \delta(k)$$

Equation 5

According to equations 5 and 6, the controller gains are a function of the forward speed of the miniature vehicle ( $V_f$ ). In other words, we have to recalculate controller gains whenever that speed changes. This is a serious problem because we must solve the Riccati equation in real time. We made use of a polynomial-fitting method to reduce the computational load. To test this controller, we executed experiments three times with different start points, as shown in Figure 8. The steady-state control errors are summarized in Table 4.

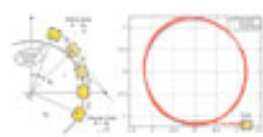


Figure 9 Circular tracking control of the vehicle

Circular tracking control causes the vehicle to track a circular line whose radius is  $R_0$ , as shown in Figure 9. To design this controller, we transformed the coordinate of Equation 4 into the polar system and linearized the equation appropriately about the circular track condition. Finally, we obtained Equation 7, which is a continuous state-space model.

The detailed derivation of Equation 7 is explained in a paper presented at ION GPS-2001 conference ("Autonomous Navigation and Control of Miniature Vehicle using Indoor Navigation System"). We also discretized Equation 7 using 0.1 second sampling time and used a DLQR method to select the controller feedback gains.

To test this controller, we made the miniature vehicle track the circle whose radius is 1.2 meters, as shown in Figure 9. The steady-state control errors for circular control are summarized in Table 5. Figure 10 incorporates a screen capture from a circular tracking demonstration video.



Figure 10 Indoor navigation system in operation

We drew a circular track on the floor using wide green tape to check visually whether the vehicle tracks the circle well. We also installed four pairs of bar gates separated by 50 centimeters across the circular track, which can be seen in Figure 10. If the system had contained small control errors, the miniature vehicle would have hit and knocked down one of these bar gates. But no impact on any bar gate occurred during more than 10 rounds of testing.



Table 4

**Conclusions and Future Work** SNUGL developed an indoor navigation system using a constellation of ceiling-mounted pseudolites. Experimental analysis showed that the horizontal point-positioning error was 0.14 centimeter (RMS) in the static case and 0.79 centimeter (RMS) in the dynamic case. For the purpose of using this system as a position and attitude sensor for vehicle control, we installed two antennas on the roof of a small test vehicle. Static error analysis showed that the horizontal positioning error was less than one centimeter (RMS) and that the attitude error was less than one degree (RMS). We also implemented cycle-slip recovery and automatic cycle-ambiguity resolution functions to make our system more robust and practical.

To check whether this is a sufficient sensor for vehicle control, we designed two controllers: simple line transfer and circular tracking. Tests of both controllers were successful - our system calculated indoor position and attitude precisely. In other words, our indoor navigation system makes it possible to use GPS techniques in such indoor environments as large factories or indoor amusement

parks, for indoor E-911, and anywhere GPS satellite signals are blocked.

$$\delta(k) = -[K_x \quad K_z] \begin{bmatrix} x_{av}(k) \\ y(k) \end{bmatrix}$$

Equation 6

In the near future, mobile European standard GSM, U.S. digital cellular CDMA standard IS-95, and 3G standard IMT-2000 hand phones may be required to include GPS modules. To make this requirement practical and inexpensive to meet, we plan to continue our research and development in this area, which will make seamless indoor/outdoor navigation possible by upgrading receivers and pseudolites.



Table 5

**Acknowledgement** This project was supported in part by a grant from the International Joint Research of the Ministry of Information & Communication, Korea and supported in part by a grant from the BK-21 program for Mechanical and Aerospace Engineering Research at Seoul National University. We would like to thank them for their support. We would like to thank Navicom Co., Ltd for providing the receivers used in our tests and for their support. c

**Manufacturers** IN-200 CXL pseudolites came from IntegriNautics, Palo Alto, California. The GPCore 1200 GPS receivers (with modified firmware) were manufactured by Navicom, Co. Ltd., Seoul, South Korea. Navicom also provided pseudolites that will become commercially available this year.

### Further Reading

- C. Kee, D. Yun, H. Jun, "Autonomous Navigation and Attitude Control of Miniature Vehicle using Indoor Navigation System," Proceedings of ION GPS-2001, Salt Lake City, Utah, September 11-14, 2001.
- C. Kee, D. Yun, H. Jun, B. Parkinson, "Precise Calibration of Pseudolite Positions In Indoor Navigation System," Proceedings of ION GPS-99, Nashville, Tennessee, September 14-17, 1999.
- C. Kee, H. Jun, D. Yun, B. Kim, Y. Kim, B. Parkinson, T. Langenstein, S. Pullen, J. Lee, "Development of Indoor Navigation System using Asynchronous Pseudolites," Proceedings of ION GPS -2000, Salt Lake City, Utah, September 19-22, 2000.
- H. S. Cobb, GPS Pseudolite: Theory, Design, and Applications. Ph.D. dissertation, Stanford University, 1997.
- J. Stone, J. Powell, "Precise Positioning Using GPS Satellites and Pseudolites for Open Pit Mining," the 4th International Symposium on Space Navigation Technology and Applications, Brisbane, Australia, July, 1999.
- K. Zimmerman, Experiments In The Use of the Global Positioning System for Space Vehicle Rendezvous. Ph.D. dissertation, Stanford University, 1996.
- Thomas Bell, Precision Robotic Control of Agricultural Vehicles On Realistic Farm Trajectories. Ph. D dissertation, Stanford University, 1999.

